

CHARACTERIZING STARTING CONDITIONS FOR HYDROTHERMAL SYSTEMS UNDERNEATH MARTIAN CRATERS. E. Pierazzo¹, N.A. Artemieva², and B.A. Ivanov², ¹Planetary Science Institute (1700 E Ft. Lowell Rd., Suite 106., Tucson, AZ 85719; betty@psi.edu), ²Institute for Dynamics of Geospheres (Russian Academy of Sciences, Leninsky pr., 38-6, 117334, Moscow, Russia; art@idg.chph.ras.ru; ivanov@idg.chph.ras.ru).

Introduction: Impact craters are widely used ubiquitous indicators for the presence of sub-surface water or ice on Mars [2]. Regardless of the state of water in the Martian subsurface, it has long been proposed [e.g., 3] that every crater of relatively large dimensions (>30 km in diameter) should have created favorable conditions for local hydrothermal activity. Rough estimates of the heat generated in impact events have been based on scaling relations [6,7], or thermal data based on terrestrial impacts on crystalline basements [8]. Preliminary studies [9,10] suggest that melt sheets and target uplift are equally important heat sources for the development of a hydrothermal system, while its lifetime depends on the volume and cooling rate of the heat source, as well as the permeability of the host rocks. Specific hydrocode simulations of impacts on a mixed ice-rock target on Mars are not yet available. We present initial results of 2D and 3D simulations of impacts on Mars aimed at constraining the initial conditions for the development of an impact-related hydrothermal system on the red planet [11]. The simulations of the early stages of impact cratering allow us to characterize the pressure-temperature distribution in the target and to evaluate the amount of shock melting caused by various impacts on the Martian surface. The late stage of crater collapse is necessary to determine the final thermal state of the target, including crater uplift, distribution of heated target material (including the melt pool) and hot ejecta around the crater.

Early stage: Simulations of the early stage of the impact event are carried out with the 3D hydrocode SOVA [12], coupled to tabular versions of the ANEOS equations of state [13]. We model spherical comets and asteroids of various sizes impacting at 15.5 and 8 km/s, respectively. These roughly correspond to median impact velocities on Mars for short-period comets and for asteroids. Simulations have been carried out for 90° (vertical), and 45° impact angles. A spatial resolution of 20 to 25 cells-per-projectile-radius is maintained over a central region around the impact point, followed by regions of progressively lower resolution. We distributed up to 500,000 Lagrangian tracers in the target, for accurate volume estimates. Tabular versions of ANEOS equations of state for basalt, water ice and granite are employed to represent target and projectile materials. A very thin CO₂ atmosphere (which is not expected to influence the thermal evolution of the target) was included in the simulations to model the present-day Martian atmosphere. In this study we address the influence of target structure (inhomogeneities) on the shock wave propagation and maximum compression. Accurate estimates of shock melting for a “wet target” cannot be determined with-

out the support of new experimental data. However, we can provide estimates of target volumes shocked to specific isobars that are reasonable thresholds for shock melting.

We carried out 3D simulations on different target configurations, starting with (A) a “dry basalt target”. Macro-scale inhomogeneities have been modeled through (B) a “layered basalt-water ice target”, with an overall percentage of 20% for water ice (“reasonable” value). Micro-scale inclusions in macro-scale cratering (*i.e.*, modeling is restricted by computer capacity) have been modeled in two different ways: (C) a “mixed cell target”, where each computational cell of the target includes two (or more) materials. In this case each cell is composed of a mixture of two materials, such as 80% basalt and 20% water ice. The hydrocode internal procedure allows for mechanical (*i.e.*, pressure) equilibrium in each cell, but not thermodynamic (temperature) equilibrium. Alternatively, wet basalt (*i.e.*, a new equation of state representing wet basalt material) can be constructed by combining the equation of state of two (or more) initial materials. We built a (D) “wet basalt target” with each cell made of a single material, 80% basalt and 20% ice, in complete mechanical and thermodynamic equilibrium.

Typical threshold pressures for shock melting of dry rocks are around 50-60 GPa [14], while for hydrous rocks localized shock melting can occur from ~30 GPa (*e.g.*, [15]; the absence of experimental data on the shock behavior of “wet basalts” does not allow us to use more precise values). We thus consider 30 to 50 GPa as the typical range for shock melting of rocks. In this range we find small differences (10 to 20%) in volume estimates of impact melt between the simulations with the dry and wet basalt (*i.e.*, mixed equation of state) as well as those with the layered target. In the basalt-ice mixed cells case, however, the volume of material shocked above a give pressure is always significantly (30 to 40%) less than in the other three cases. This may be indicative of different thermodynamic effects involved when two materials are mixed together in individual target cells compared to uniform material cells. In general, the mixed cell case (C) results in overall lower values of shock compression, but manifests regions of “heat concentration” (*i.e.*, cells with higher temperatures) for materials with lower impedance. It is not clear to us what is the best modeling approach for mixed materials targets (both approaches, mixed cells and mixed material equation of state, have been used in modeling studies). The mixed cells approach (case C) lacks thermodynamic equilibrium in individual computational cells, but allows us to see a separation between water and basalt in the vapor

plume. The uniform target case (case D) achieves mechanical and thermodynamic equilibria within each computational cell, but at any instant the vapor plume consists of wet basalt of constant (*i.e.*, 20%) water content, which is unrealistic.

Melt production is also affected by impact characteristics. While the difference in shocked volume between vertical and 45° impacts appears minimal, impact velocity has a significant effect on the total volume of possible melt, Figure 1. The typically higher impact velocities of cometary impacts results in melt volumes that may be two to three times larger than asteroid impacts at constant crater size. Larger melt pools have longer cooling times and may contribute to a longer duration of the hydrothermal system.

Late Stage: For the late stage modeling we use the pure water/ice phase diagram to identify the potentially stable phase of water associated with the thermal state underneath the crater (providing that the pore water has the same temperature as the surrounding material). Figure 2 shows the resulting thermal fields underneath the transient and final crater created by asteroid (upper) and comet (lower) impacts in a dry target. Both modeled craters suggest the same general picture: The combination of shock/plastic heating and the structural uplift of initially deeper strata create a region under the crater where liquid water is stable. Heating comes mainly from the shock wave propagation combined with the structural uplift of rocks underneath the crater; deviatoric stresses (mostly friction from disrupted rocks) contribute a maximum of ~100K to the heating, mainly near the surface, under the crater center. The main difference between asteroid and cometary impacts consists in a larger volume of hot rocks in the central peak of the comet-produced crater. This is a natural result of higher initial shock pressures near the impact point due to the higher impact velocity. In the central uplift the high temperatures cause water to evaporate (steam-driven circulation). The liquid and

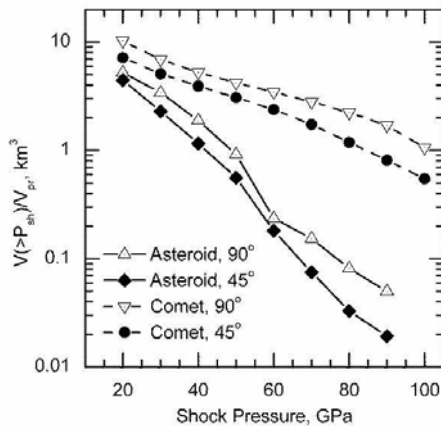


Figure 1: Volume of target subject to shock pressures above a given value normalized to projectile volume for asteroidal and cometary impacts and different impact angles (45°, 90°) on a mixed cell target (case C).

vapor water stability zone identify the hydrothermal circulation cell. Figure 2 shows that for a mid-sized crater (rim diameter ~30 km) in an arid region of Mars any hydrothermal circulation is probably restricted to a “column” contained well within the final crater. These initial models provide crater shapes that are in reasonable agreement with MOLA data for fresh mid-size craters. Work is in progress to develop a strength model for a mixed rock-ice target based on available mechanical properties of dry basalt, ice, and permafrost.

This work is supported by NASA Grant NAG5-12688.

References: [1] Squyres S.W. et al., (1992) in *Mars*, Kieffer, Jakosky, Snyder, Matthews, Eds., Tucson Arizona Press. 523. [2] Newsom H.E. (1980) *Icarus*, 44, 207. [3] Corliss J.B. et al. (1981) *Ocean. Acta, SP*, 59. [4] Farmer J. (1996) in *Evolution of hydrothermal ecosystems on Earth (and Mars?)*, Bock, Goode, Eds. (Wiley, New York), 273. [5] Newsom H.E. et al. (2001) *Astrobiol.*, 1, 71. [6] Grieve R.A.F., Cintala M.J. (1992) *Meteoritics*, 27, 526. [7] Clifford S.M. (1993) *J. Geophys. Res.*, 98, 10973. [8] Ivanov B.A., Deutsch A. (1999) *GSA Spec. Pap.* 339, 389. [9] Daubar I.J., Kring D.A. (2001) *LPSC*, 32, #1727. [10] Thorsos I.E. et al. (2001) *LPSC*, 32, #2011. [11] Pierazzo E. et al. (2005) *GSA Special Paper* 384. In Press. [12] Shuvalov V. (1999) *Shock waves*, 9, 381. [13] Thompson S.L., Lauson H.S. (1972) *SC-RR-61 0714*, Sandia Nat. Labs. [14] Stöffler D. (1984) *J. non-Cryst. Sol.* 67, 465. [15] Lambert P., Lange M.A.

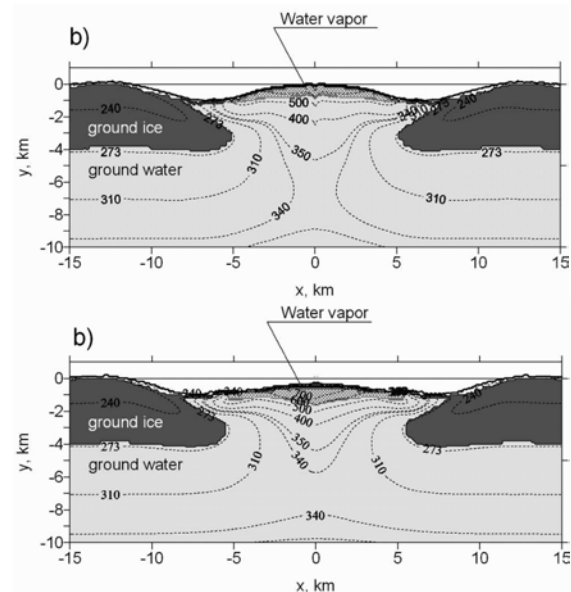


Figure 2: Isotherms and phase state of pore water (relative to local temperatures and pressures) below a Martian crater with rim diameter of ~30 km formed by an asteroid (upper) and a comet (lower) impact. Ice: dark gray; water: light gray. Regions of water vapor stability are cross-hatched. Lithostatic pressure increases the boiling point. Consequently, liquid water may exist at a temperature up to the critical point (650 K) below the central peak.

(1984) *J. non-Cryst. Sol.* 67, 521.